Space view issues for hyperspectral sounders

Evan M. Manning*, Hartmut H. Aumann, and Steven E. Broberg
Jet Propulsion Laboratory, 4800 Oak Grove Dr., Pasadena, CA 91109

ABSTRACT

The expectation for climate quality measurements from hyperspectral sounders is absolute calibration accuracy at the 100 mK level and stability at the < 40 mK/decade level. The Atmospheric InfraRed Sounder (AIRS)[1], Cross-track Infrared Sounder (CrIS), and Infrared Atmospheric Sounding Interferometer (IASI) hyperspectral sounders currently in orbit have been shown to agree well over most of their brightness temperature range. Some larger discrepancies are seen, however, at the coldest scene temperatures, such as those seen in Antarctic winter and deep convective clouds. A key limiting factor for the calibrated scene radiance accuracy for cold scenes is how well the effective radiance of the cold space view pertains to the scene views. The spaceview signal is composed of external sources and instrument thermal emission at about 270 K from the scan mirror, external baffles, etc. Any difference in any of these contributions between spaceviews and scene views will impact the absolute calibration accuracy, and the impact can be critical for cold scenes. Any change over time in these will show up as an apparent trend in calibrated radiances. We use AIRS data to investigate the validity of the spaceview assumption in view of the 100 mK accuracy and 40 mK/decade trend expectations. We show that the space views used for the cold calibration point for AIRS v5 Level-1B products meet these standards except under special circumstances and that AIRS v6 Level-1B products will meet them under all circumstances. This analysis also shows the value of having multiple distinct space views to give operational redundancy and analytic data, and that reaching climate quality requires continuing monitoring of aging instruments and adjustment of calibration.

Keywords: AIRS, climate quality, spaceview, calibration, trends

1. INTRODUCTION

Some of the earliest and most important impacts of climate change are found in polar regions. But the accuracy and stability of the absolute calibration of the spaceborne instruments used to monitor climate is usually monitored in space relative to tropical ocean surface temperatures, which are measured directly by floating buoys. These temperatures are typically ~300 K. For AIRS we have placed an limit on the trend of less than 60 mK/decade[2]. This performance approaches the standards for climate quality from Ohring et al.[3,4] of 100 mK absolute accuracy and 40 mK/decade of stability. However, the observed limits on AIRS trends at 300 K cannot be assumed to be applicable to measurements at 250 K and colder. For 900 cm^{-1} the radiance at 210 K is a factor of ten smaller than at 300 K. This makes the calibration for cold scenes much more sensitive to the accuracy and stability of the zero point value, which is derived from multiple views of space. The key areas where AIRS, CrIS, and IASI observe cold scenes are polar regions and cold clouds.

We now show interesting trends from AIRS and IASI in polar data and analyze the sensitivity of the calibration to the quality of the space views (SVs). We next test the quality of the SVs, first using lunar roll data, then with a global analysis of the spaceview data set.

1.1 Polar example

AIRS and IASI are both in polar orbits. AIRS on Aqua has a 1:30 PM ascending equator crossing while IASI on MetOp-A has a 10:30 AM crossing. So they view the tropical and temperate regions of Earth at different local times. However, both cross each pole every ~100 minutes, so there is a wealth of comparison data. For this study we take daily

* Evan.M.Manning@jpl.nasa.gov ; phone 818-354-1172

samples of polar (|latitude| > 68 degrees) nadir data at 2616 cm^{-1} from each instrument, as daily averages from 2007-2013. For each instrument and pole we first calculate and remove a seasonal cycle, leaving an anomaly.

2616 cm^{-1} is a window channel near the shortwave end of the range of AIRS. For IASI we synthesize an analogous channel from multiple window channels in 2600-2650 cm^{-1}.

Figures 1 and 2 show AIRS and IASI anomalies for Arctic (~260 K) and Antarctic (~245 K) regions.

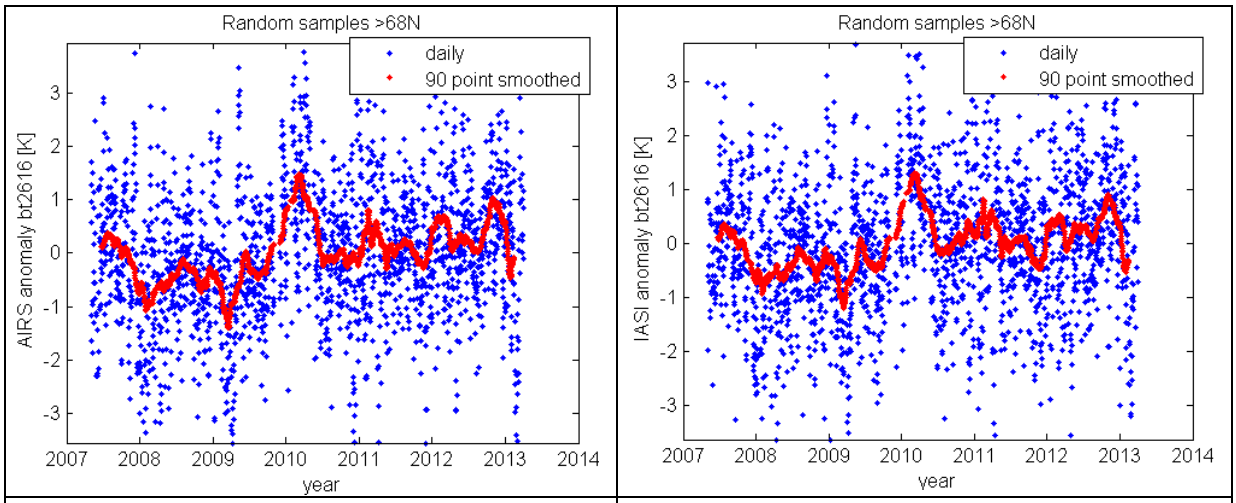

AIRS shows warming at 1370 +/- 180 mK/decade	IASI shows warming at +1050 +/- 200 mK/decade

Figure 1. AIRS and IASI Arctic anomalies for 2007-2013 with 90-point smoothing.

For the entire Arctic region (lat > 68 N), both AIRS and IASI show large and statistically significant trends, but the trends are not significantly different.

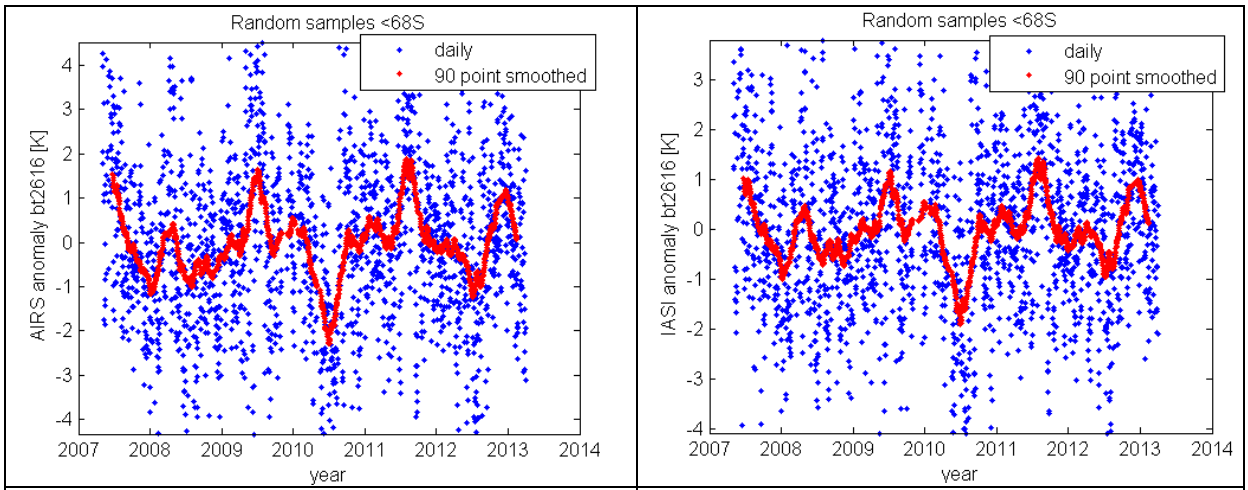

AIRS anomaly trend +160 +/- 230 mK/decade	IASI anomaly trend +150 +/- 220 mK/decade

Figure 2. AIRS and IASI Antarctic anomalies for 2007-2013 with 90-point smoothing.

For the Antarctic IASI and AIRS trends are much smaller than for the Arctic, but again the two instruments agree.

The observed trends from the two instruments agree very well in both polar regions. These trends will be of interest for climate, but first we must eliminate the possibility that the trends are spurious.

1.2 Space View Analysis

Infrared radiometers are calibrated by periodically viewing an Onboard Blackbody Calibrator (OBC, typically near 300 K) and by pointing the instrument at cold space for a Space View (SV). Radiometric calibration of science observations then consists of interpolating between the hot and cold signal levels to match the science signal. This is illustrated in Figure 3. Additional adjustments are made to account for such effects as detector nonlinearity and polarization. What is measured in the OBC view is the OBC + Instrument Thermal Emission (ITE), in the SV we measure deep space (2.7 K) + ITE + External Signal (XS) and in the scene view we measure the Earth scene thermal emission + ITE + XS. In the calibration the XS is assumed to be neglible and the ITE cancels in theory. However, the instrument optical configuration is not exactly the same when viewing the OBC and SV as it is when viewing Earth scenes, i.e. the ITE_{sv}, ITE_{earth} and ITE_{obc} are not exactly the same and XS_{SV} and XS_{Earth} may be nonnegligible. Most of these effects are measured during the prelaunch calibration. Due to local differences in the accumulation of contamination on the various instrument surfaces which are seen in the sidelobes of the instrument beam, the balance between ITE_{sv}+XS_{SV}, ITE_{earth}+XS_{Earth} and ITE_{obc} may shift. This could create a trend artifact in the data. If not recognized this artifact may be mistaken as a measurement of climate change.

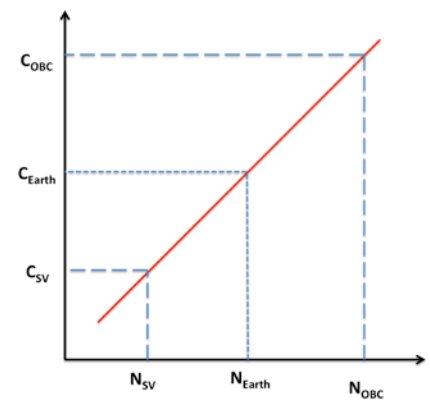

Figure 3. Simplified radiometric calibration. When the instrument observes space (SV) and a hot blackbody (OBC), downlinked counts C_{SV} and C_{OBC} correspond to known radiances N_{SV} and N_{OBC}. This gives a linear fit that yields an Earth scene radiance N_{Earth} for any downlinked C_{Earth}.

Table 1 shows the error in mK introduced at various frequencies and scene brightness temperatures if the cold or hot targets have an error where 0.1% of the correct signal is replaced by a signal from a 250 K source, perhaps part of the instrument. Table 2 shows the same thing for a 0.1% of 250 K leak into the hot target.

Table 1. Error in mK introduced into science observations at various frequencies and scene brightness temperatures by a leak of 0.1% of 250 K radiance into the cold reference.

Frequency	180 K	200 K	220 K	240 K	260 K	280 K	300 K
650 cm^{-1}	134	89	61	42	27	15	4
800 cm^{-1}	158	96	61	40	24	13	3
1000 cm^{-1}	203	108	62	37	22	11	3
1200 cm^{-1}	269	124	64	35	19	9	2
1400 cm^{-1}	362	144	67	34	17	8	2
1600 cm^{-1}	496	170	70	32	15	7	2
2200 cm^{-1}	1328	295	84	29	11	4	1
2600 cm^{-1}	2548	442	98	28	9	3	1

Table 2. Error in mK introduced into science observations at various frequencies and scene brightness temperatures by a leak of 0.1% of 250 K radiance into the hot reference.

Frequency	180 K	200 K	220 K	240 K	260 K	280 K	300 K
650 cm^{-1}	18	22	26	31	36	42	48
800 cm^{-1}	16	20	24	29	34	39	45
1000 cm^{-1}	15	18	22	27	31	36	41
1200 cm^{-1}	14	17	20	24	28	33	38
1400 cm^{-1}	13	16	19	22	26	30	35
1600 cm^{-1}	12	14	17	21	24	28	32
2200 cm^{-1}	9	11	14	17	19	22	26
2600 cm^{-1}	8	10	12	14	17	20	23

From measurements of the sea surface temperature (SST) at 300 K we know that the instrument is stable at the better than 60 mK/decade level for typical 300 K SST views. But what can we say about the stability at cold temperatures? From Table 2 we can see that the effect of a leak into the hot reference (OBC) decreases as the scene temperature decreases. At 2600 cm^{-1} the effect at 240 K is 14/23 ~= 60% of the effect at 300 K. So a leak that would cause the 60 mK/decade of false trend at 300 K would only cause ~35 mK/decade of false trend at 240 K. But from Table 1 we can see that a leak at the cold reference would have almost no effect at 300 K, so the 60 mK/decade measurement at 300 K is no guarantee of accuracy at cold scene temperatures. The effect of a leak into the cold reference is even stronger at colder scene temperatures, such as the ~210 K seen in deep convective clouds, especially at the shortest wavelengths. A different approach is needed to detect changes in ITE_{sv} and XS_{SV} in AIRS data, which is described below.

The AIRS instrument has four spaceview samples at four different angles and observes all four each scan. This presents a great opportunity to investigate ITE_{sv} and XS_{SV} using on-orbit data, because any problems with the SVs are unlikely to be uniform over the four SVs. The first possible problem we wish to investigate is limb contamination. The first two SV samples (SVA and SVB) angle downwards from the spacecraft and so may be too close to the Earth, i.e. XS_{SVA} and XS_{SVB} may be contaminated from Earth's limb.

The spaceviews are centered at angles of {75, 83, 92, 101} degrees from nadir. Table 3 shows the locations of these spaceviews, and the lowest altitude of any contribution. During spaceviews the scan mirror is scanning at a rapid and changing rate, so values are also provided for the low edge of the spaceviews. Numbers for the low edge are only approximate because the edge is not perfectly sharp and different individual detectors have different response at the extremes. The instrument was designed so that all spaceviews would not get any signal from within 100 km of Earth's surface, under the assumption that above this altitude there will be no significant atmospheric signal.

Table 3. Geometry of AIRS spaceviews with respect to Earth's limb near the South Pole. '(730)' denotes rays that look upwards from the Aqua spacecraft's 730 km altitude, so in these cases 730 km is the lowest altitude, but is not a tangent point.

	Center scan angle (degrees from nadir)	Height of lowest approach to Earth for center scan angle (km)	Lowest scan angle (degrees from nadir)	Height of lowest approach to Earth for lowest scan angle
Spaceview A (SVA)	75	474	69	244
Spaceview B (SVB)	83	662	78	560
Spaceview C (SVC)	92	(730)	87	705
Spaceview D (SVD)	101	(730)	97	(730)

The 2378 AIRS channels each have their own individual detectors and electronics up to the Analog-to-Digital converter. These detectors are grouped in 17 modules, with the detectors within a module sharing the same grating order and optical path. Filter and instrument polarization add a 2*scan_angle modulation to the zero level, which creates differences in signal levels among the spaceviews even when they all view the same cold space. Patterns of polarization are similar within each module but vary strongly between modules. Module frequencies are listed in Table 5, below.

Some detector modules have zero levels that drift, so every 20 minutes they are reset to a baseline level with a "DC Restore". DC Restores are handled well in the operational v5.0 Level-1B calibration software, but they complicate analysis of spaceview differences, so cases with DC Restores are avoided in these analyses.

2. RESULTS

2.1 Lunar roll data set

The Aqua spacecraft on which the AIRS instrument is carried makes monthly maneuvers so that the MODIS instrument can use the moon as a calibration source. During these maneuvers the Aqua spacecraft is rolled by 0.2-20 degrees as required for MODIS. AIRS also observes the moon in its last spaceview during these maneuvers, but that is not the emphasis here. During the roll the last few science observations from AIRS are moved onto Earth's limb and beyond. The spaceviews are moved farther from Earth than their nominal locations.

Here we use data from a maneuver on July 2, 2009, when the Aqua spacecraft was held at an angle of 19.75 degrees for about 7 minutes.

AIRS performs a continuous scan through 90 Earth scene fields of view (FOVs) with nominal centers -49 to +49. The FOV separation and spatial extent are both 1.1 degrees, so the edge of the source of signal for one FOV is the center of the next one. Table 4 gives the geometry during the roll.

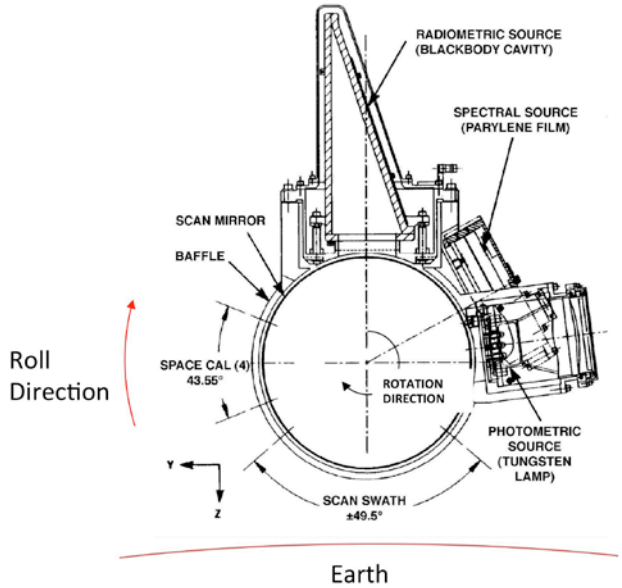

Figure 4. AIRS scan geometry

Table 4. Geometry of AIRS FOVs with respect to Earth's limb during the 2009-07-02 roll.

FOV #	Scan angle (degrees from nominal nadir in instrument frame)	Nadir angle (degrees from actual nadir during 19.75 degree roll)	Height of lowest approach to Earth (km)	Comment
45	-0.6	20		Typical Earth scene
85	-43.4	63.2	-34	Limb darkening
86	-44.5	64.3	26	Stratospheric emission
87	-45.6	65.4	84	Stratospheric emission in a few bands
88	-46.7	66.5	140	Space
89	-47.8	67.6	193	Space
90	-48.9	68.7	244	Space

Figure 5 provides images of the scene data during this time for selected channels. In these images the vertical axis tracks the direction of travel and the FOVs that include the limb and space are on the right edge. The top row shows the entire extent of the data set: 166 scans by 90 FOVs. The second row zooms in on the upper right corner of the images to show limb behavior. Signal for space is essentially zero and blue pixels show where instrument noise pushes the signal below 0 K.

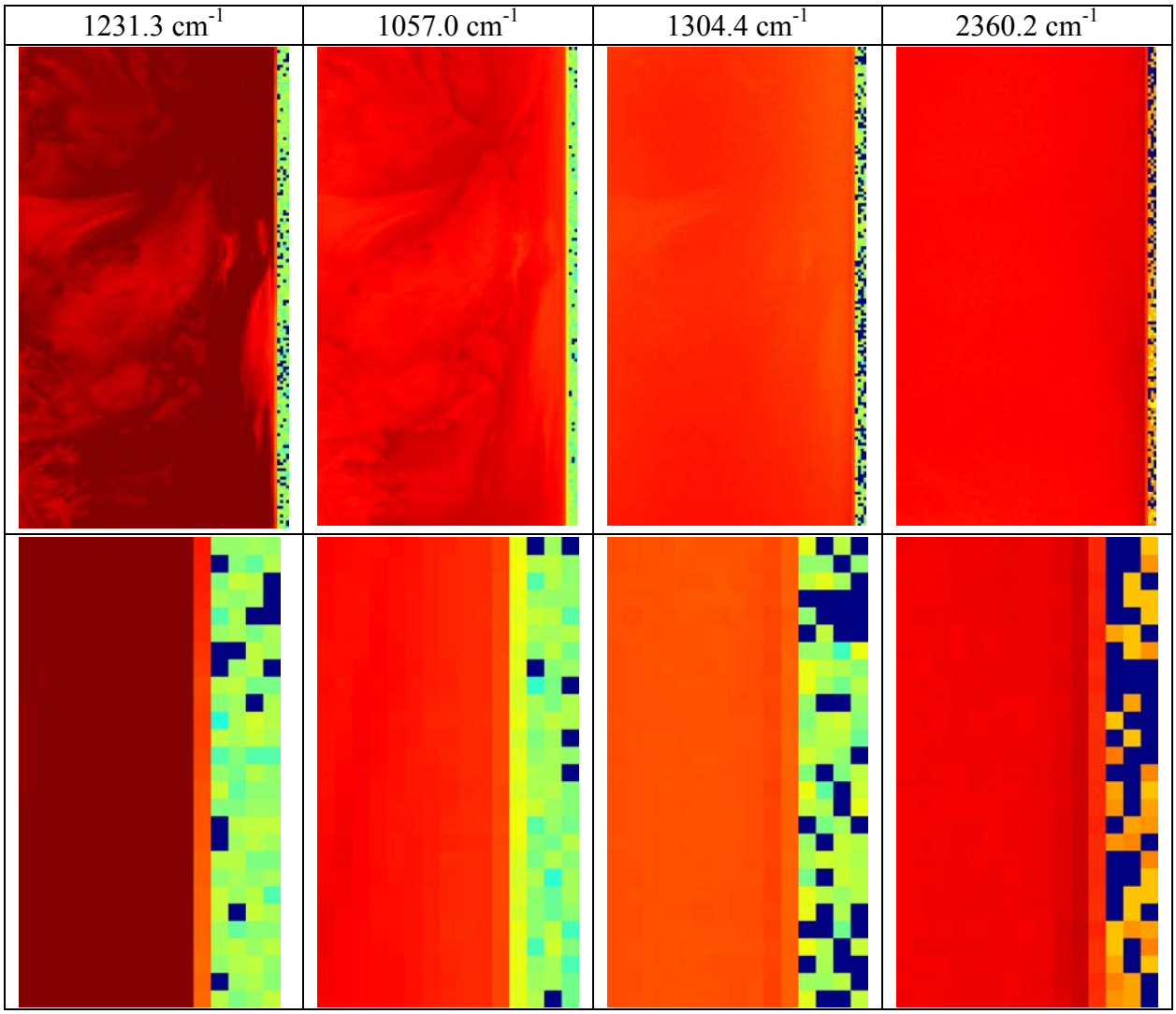

Figure 5. Images of scene views during roll maneuver.

The first column of images in Figure 5 shows a typical window channel with surface and cloud structure visible. The last 4 columns of FOVs in those images, corresponding to FOVs 87-90, look as cold as space. The preceding FOV, FOV 86, is bright with atmospheric emission.

The second column of images in Figure 5 shows an ozone channel with peak sensitivity at nadir near 47 hPa. Surface features are washed out and only FOVs 88-90 are as cold as space.

The 3rd column of images in Figure 5 shows a methane channel. Surface and atmospheric features are almost absent but it darkens in FOV 85 toward the limb then brightens in FOV 86 with stratospheric emission. FOVs 87-90 are cold as space.

The last column of images in Figure 5 shows a stratospheric CO_2 channel with peak sensitivity at nadir near 7 hPa. It darkens in FOVs 85-86 toward the limb then brightens in FOV 87 with stratospheric emission. FOVs 88-90 are cold as space.

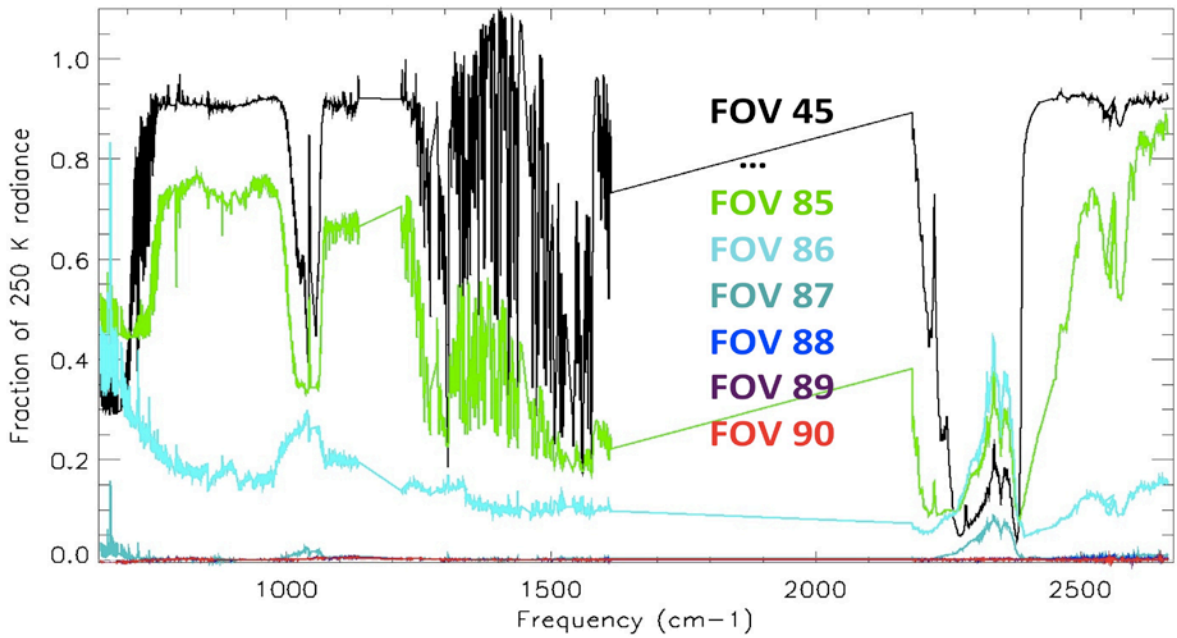

Figure 6. Spectra for space and limb spectra during roll maneuver. Units are fraction of 250 K radiance.

Figure 6 shows mean spectra by FOV#, as a fraction of the radiance corresponding to 250 K. FOV 85 shows significant limb darkening but is still basically an Earth spectrum. FOV 86 shows only atmospheric emission. FOV 87 is cold as space except in a few emission bands. FOVs 88, 89, and 90 show no significant signal. Since the lowest edge of the lowest spaceview during normal operations corresponds to the location of FOV 90 during this maneuver, it appears that the spaceviews are free from limb contamination, or at least that any limb contamination did not exceed ~0.01 on the scale of fraction of 250 K radiance near the south pole in July 2009.

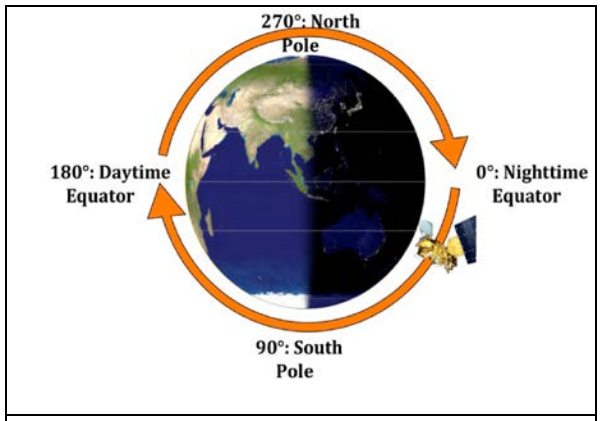

Figure 7. Orbital phase illustrated.

2.2 Global spaceview data set

While it is encouraging that no limb contamination was seen with the roll data set, the statistical power of that analysis is limited by the fact that it represents only a small amount of data. In addition, it represents only one specific observation time, and so could miss effects specific to orbital, seasonal, and long-term changes. There could also be contamination in spaceviews from sources other than the Earth's limb.

To investigate further, we look at statistics of spaceviews taken during normal instrument operations, specifically the differences in signal levels among the 4 spaceviews. Means per 6-minute granule of these differences are collected in the AIRS Level-1B field "input_space_signals.mean". For this analysis we first make monthly averages of this quantity, binned into 24 15-degree bins by "orbital phase". Orbital phase is a metric of where the observations were taken in the orbital cycle of the Aqua platform. Figure 7 shows the definition of orbital phase.

Data are collected throughout each month whenever the instrument is in science mode, but excluding the 30% of granules containing DC Restores. The monthly mean of each bin is thus the result of approximately 30,000 observations, compared to 166 observations in the roll data set. The use of this much data makes this analysis statistically strong, able to distinguish effects far smaller than the instrument noise level.

Because of polarization effects, even in the absence of any contamination we do not expect equal signal levels from the 4 space views. Instead we expect patterns of differences which can be fit with a simple sinusoidal function of 2 * scan_angle. Figure 8 shows global mean relative signal level (in instrument counts) for averages of the 30 best channels per detector module as a function of scan angle, along with a best-fit curve. We see that on average the fit is very good, indicating very little contamination.

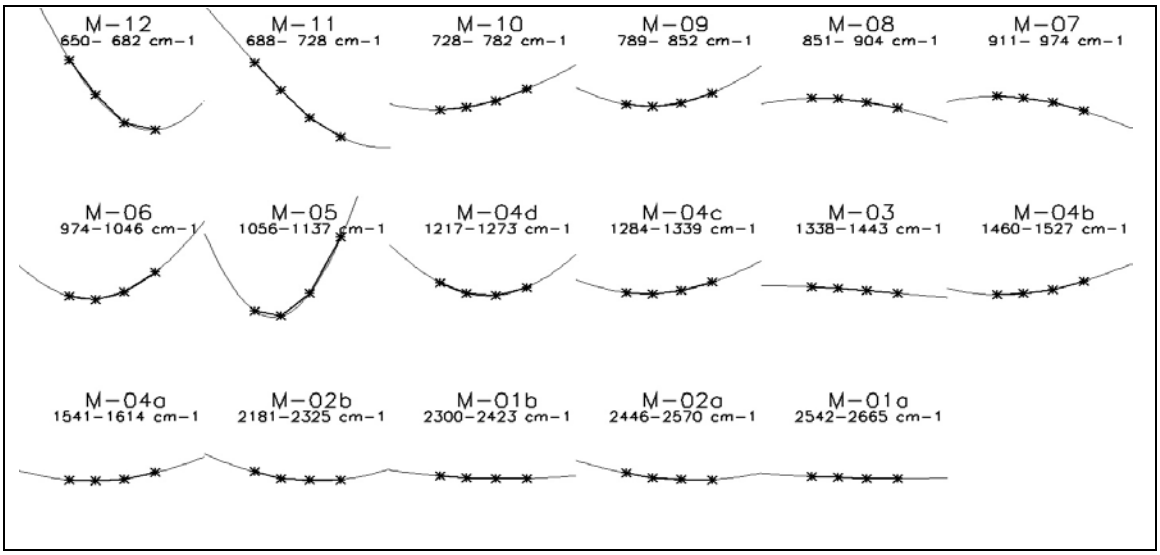

Figure 8. Global counts vs. angle for 4 spaceviews by detector module, with best-fit polarization curves

But the picture gets more complicated when we separate out the results into 15-degree orbital phase bins as shown in Figure 9. We see that for a small part of each orbit, the near-Earth space views are significantly elevated, with the amount of the effect varying strongly with module, but generally stronger at the shortwave end of the spectrum.

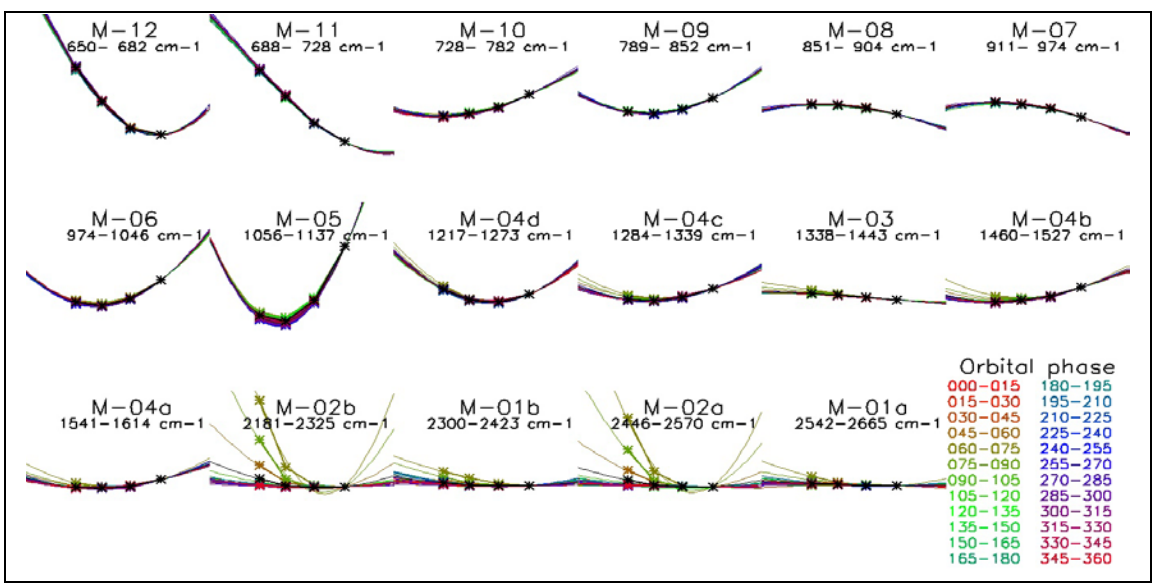

Figure 9. Counts vs. angle for 4 spaceviews by detector module, with best-fit polarization curves, as in Figure 8. Figure 9 adds differently colored lines for each orbital phase angle bin. The orbital phase range for each color is shown in the lower right corner of the figure.

Since the problem looks like an excess of signal in the near-Earth space view(s), for the next figures we define a metric SV_exceedance, which is the excess signal in the near-Earth spaceview compared to the farthest spaceview, after subtracting the orbital median value.

Figure 10 shows the orbital patterns for all 17 detector modules. In Figure 10a, the scale is 1% of the radiance of a 250 K blackbody. All that shows up at this scale are rises near 70 degrees of orbital phase, which is when the spacecraft is approaching the South Pole and crossing from dark to light. In Figure 10b the scale is increased to +/- 0.02% of 250 K radiance and orbital structure is evident in most modules. All modules M-04d - M-01a have the same peak near 80 degrees but at lower magnitudes. Several also show a much smaller peak centered near 180 degrees of orbital phase. M-05 has a clear orbital sinusoid, and some of the other modules have a weaker version of this.

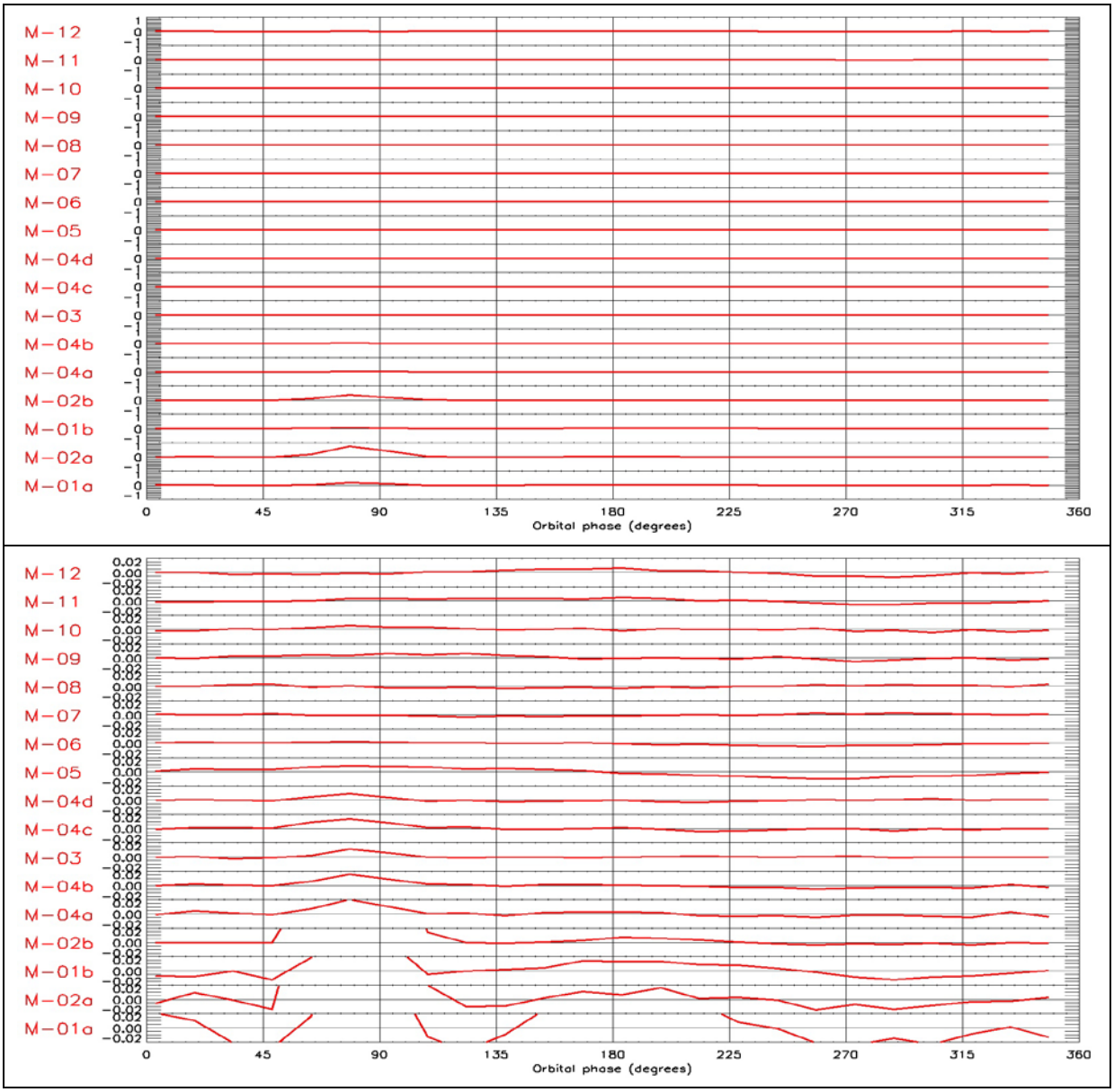

Figure 10. The orbital patterns of near-Earth spaceview excess for all 17 detector modules as a function of orbital phase. a) Full vertical scale (+/- 1% of 250 K radiance). b) Vertical scale zoomed to 0.02% of 250 K.

The magnitude of the largest SV_exceedance is ~1% of 250 K for module M-02a. The calibration software uses a median of the 4 spaceviews and the second-largest SV_exceedance is only ~0.2% of 250 K, therefore the impact on the zero-point for calibration is ~0.1% of 250 K radiance. From Table 1 we see that the impact in the 2500 cm^{-1} wavenumber region of M-02a can be as high as ~2 K for a 180 K scene but drops rapidly with rising scene temperature and is ~100 mK even for a 220 K scene. This magnitude of error will be noticed only for very specific studies looking at the coldest scenes in this particular Antarctic region with these wavelengths. Impacts for other modules are even smaller.

The figures so far have looked at statistics over 6-minute granule averages, which is the best that can be done with the Level-1B product. To investigate the fine-scale temporal/phase behavior, we now look at statistics taken from Level-1A data, where the original data is available at 2.667 second temporal resolution. Figures 11 and 12 show smoothed SV counts for module M-02a relative to a constant baseline as a function of orbital phase angle.

Figure 11 also shows some other lumps, which are largest in orbits 3 and 10. In these events all 4 SVs rise together and in fact so does the OBC (not shown). This is a rise in the baseline level associated with the South Atlantic Anomaly (SAA). Because all calibration and scene observations are equally affected, this effect calibrates out perfectly, with no impact on resulting radiances.

With the daily means at the bottom of figure 11 and on figure 12, we can now fully resolve the fine-scale behavior of the artifact around 80 degrees of orbital phase, which has a distinctive 2-lobed shape. We can see that the second SV from Earth (blue) is also affected. This is important because the calibration uses a median of the 4 SVs, so if only one SV was affected then there might be no impact on calibrated radiances.

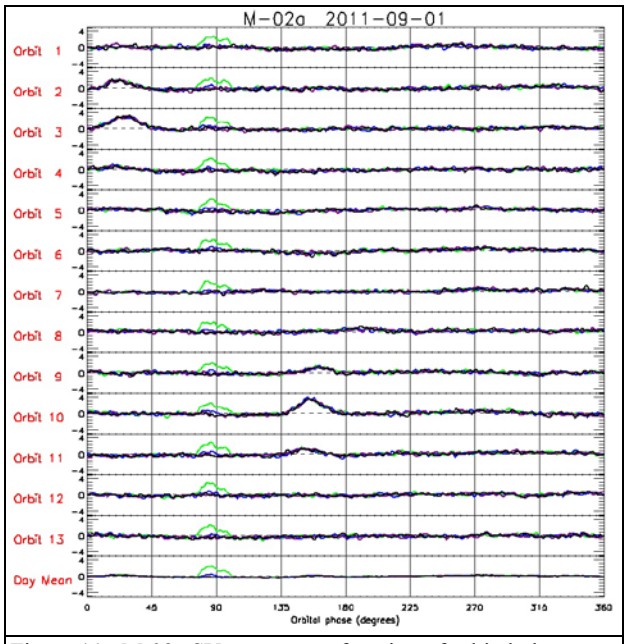

Figure 11. M-02a SV counts as a function of orbital phase angle. Orbit-by-orbit spaceview counts for 2011-09-01 with daily mean. Green is closest to Earth, then blue, purple, and black.

From Figure 12a we see that the size of the effect has grown over the mission but has leveled off after 2009 and may be decreasing.

From Figure 12b we see that the position of the peak moves relative to the Earth with a seasonal cycle. It apparently stays in a constant position in the Earth-sun-spacecraft system, where the spacecraft emerges from eclipse into sunlight. There is also an interesting seasonal variation in the shape of the peak. In the graph for 2009-06-01 there is an additional signal because the moon intruded into 2 of the spaceviews during this day. Moon-impacted spaceviews are automatically excluded in the calibration so radiances are not affected.

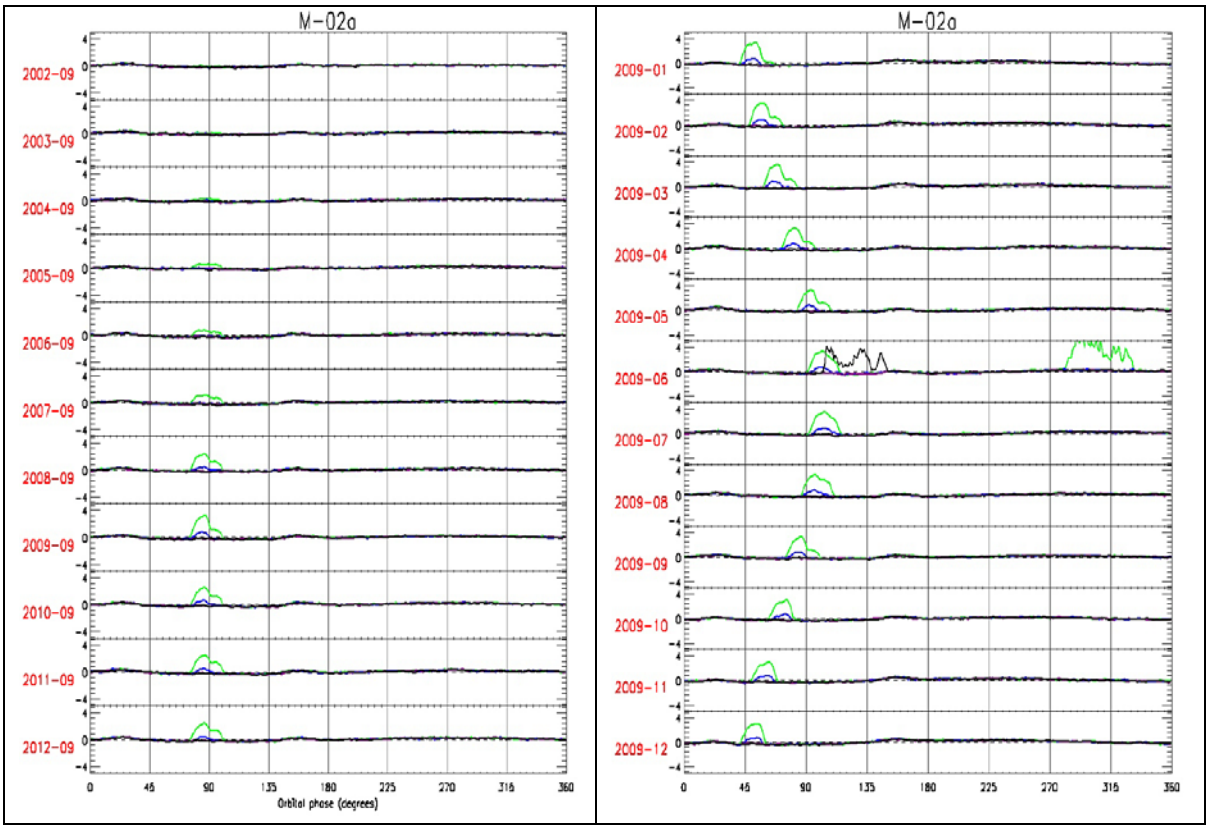

Figure 12. M-02a daily mean SV counts as a function of orbital phase angle. Green is closest to Earth, then blue, purple, and black. a) Daily means for September 1 of 2002-2012. b) Daily means for the first day of each month in 2009.

Finally, we want to see whether the effect is observable in the calibrated radiances. The effect is very difficult to observe because it is so much smaller than scene variability and even smaller than instrument noise. But there is an opportunity afforded by overlaps in spectral coverage between modules M-01b and M-02b and also modules M-01a and M-02a. In each case the channels in the two modules do not match perfectly, so we take a mean over the M-01x channels in the overlap region and then use a regression to calculate weights for the M-02x channels to get the best match. There are residual errors from the imperfect response match, but the expected feature near 80 degrees orbital phase is clear in Figure 13.

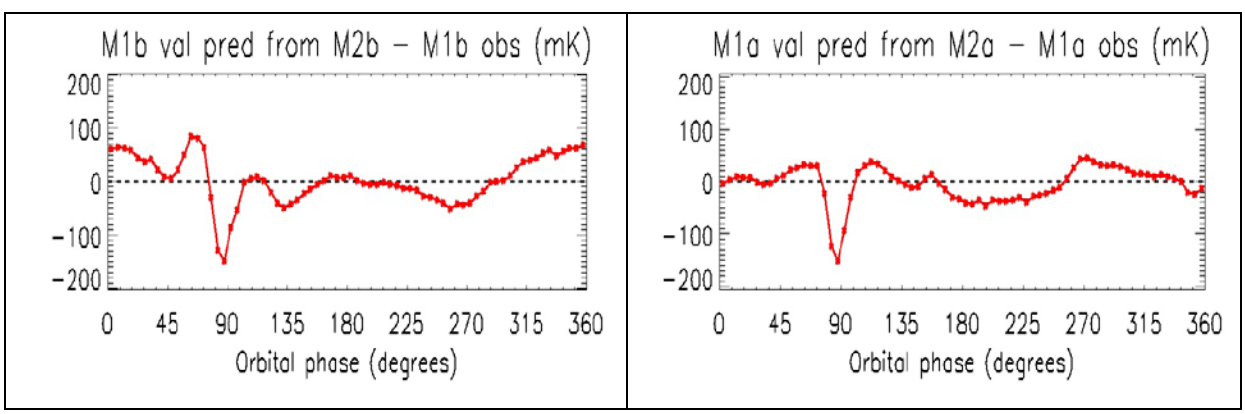

Figure 13. M1/M2 overlap mismatch in scene data for September 1, 2011. Units are mK at local mean scene temperature. a) M-02b vs. M-01b. b) M-02a vs. M-01a.

Table 5. AIRS detector modules

M-12	650-682 cm^{-1}
M-11	688-728 cm^{-1}
M-10	728-782 cm^{-1}
M-09	789-852 cm^{-1}
M-08	851-904 cm^{-1}
M-07	911-974 cm^{-1}
M-06	974-1076 cm^{-1}
M-05	1056-1137 cm^{-1}
M-04d	1217-1273 cm^{-1}
M-04c	1284-1399 cm^{-1}
M-03	1338-1443 cm^{-1}
M-04b	1460-1527 cm^{-1}
M-04a	1541-1614 cm^{-1}
M-02b	2181-2325 cm^{-1}
M-01b	2300-2423 cm^{-1}
M-02a	2446-2570 cm^{-1}
M-01a	2542-2665 cm^{-1}

Climate quality is taken to mean 100 mK of absolute accuracy and less than 40 mK/decade of trend. The effects discussed here are much smaller than this except for M-02a and M-02b in a narrow band of Antarctica. Errors here cause the reported M-02x radiances to be up to ~150 mK colder than they should be. Most scientific analyses probably would pool data from a larger area and therefore dilute the effect below the 100 mK threshold.

In terms of trend, this effect grew from ~0 to ~150 mK during the decade, so its rate is 150 mK/decade. This violates the 40 mK/decade criterion but again would be seen only in very focused analyses.

In AIRS v6 Level-2 software, channels in M-02b are used only in retrieving carbon monoxide, and channels in M-02a are used only in retrieving shortwave surface emissivity. For reasons unrelated to the artifact, retrievals of these quantities are poor in the Antarctic region where this artifact is found, and no anomaly in the Level-2 products seems linked to this artifact.

3. DISCUSSION

The 1% of 250 K radiance effect seen in the global data set approximates the 1% limit for limb contamination from analysis of the roll data. The effect seen in spectrally resolved global data (not shown) doesn't have the spectral structure of emission bands seen in limb data. Instead it is spectrally flat within modules with abrupt discontinuities at module boundaries. Together with the observation that the effect is seen in the second FOV from Earth as well as the first, this suggests that the source of the signal is not limb contamination.

The way the effect varies discontinuously on module boundaries means that instrument architecture plays some role. Some glint or sidelobe affects modules M-02a and M-02b (which share some optics) more than M-01b, even though M-01b is spectrally between the two M-02 modules.

If the warming trends seen in polar regions (Figures 1 & 2) are due to a shift of the zero point, the zero point would have to get colder, thus increasing the apparent signal from cold sources. The zero-point shift would also have to be much larger for the Arctic than the Antarctic, about -1000 mK/decade in the Arctic and -150 mK/decade in the Antarctic @ 2616 cm^{-1}, which is part of AIRS module M-01a. The largest trend seen from spaceview contamination is +150 mK/decade, but only for a section of the Antarctic and only for instruments modules M-02a and M-02b. If the spaceview contamination trend effect is ~1/5 the size for M-01a as for M-02a and if averaging over all of Antarctica reduces the effect by a factor of 2, then the spurious trend for Antarctica at 2616 cm^{-1} would be ~+15 mK/decade, an order of magnitude smaller than both the observed trend and the uncertainty on that trend.

The contamination effect in the spaceview closest to Earth can easily be removed by modifying the calibration algorithm to exclude the affected spaceviews. One or two spaceviews nearest Earth could be excluded statically, or they could be excluded dynamically when the effect is predicted or when it is detected. Using fewer space observations will slightly increase noise levels, so some adjustment to the smoothing of space views may be needed to compensate.

We have carefully analyzed the potential impact of this unexpected feature of AIRS spaceviews for Antarctic shortwave radiances. Its worst-case magnitude was shown to be 150 mK absolute or 150 mK/decade. The flip side is that AIRS data is generally free of spaceview-caused biases or trends. The lack of any spaceview problem of the magnitude of the AIRS and IASI polar trends supports the hypothesis that these trends are real.

This case study suggests these lessons learned which might be helpful to designers and operators of other instruments:

1. Calibration for cold scenes depends much more strongly on spaceview integrity than does calibration for warm scenes.

2. Having multiple distinct spaceviews is very useful. Operationally, the extra spaceviews allowed the calibration to greatly reduce the magnitude of this unexpected contamination. The problem would also have been much harder to identify and analyze with only one spaceview location.
3. Don't assume instruments are static in orbit. The artifact discussed here was not found in early-mission testing because it had not yet manifested.
4. Reaching the 40 mK/decade climate quality target will require careful monitoring of the instrument as it ages and treating some instrument parameters as functions of time. For AIRS, parameters that might change include detector and electronic nonlinearity, OBC emissivity, and mirror optical properties.
5. It might be helpful for future instruments to add a blackbody at a temperature between 0 K space and 300 K warm calibration target for use in tracking the sort of effects discussed here.

ACKNOWLEDGEMENTS

The research described in this paper was performed at JPL and was funded by NASA. The Jet Propulsion Laboratory is operated by California Institute of Technology under NASA contract.

REFERENCES

[1] Aumann, H. H., Chahine, M. T., Gautier, C., Goldberg, M., Kalnay, E., McMillin, L., Revercomb, H., Rosenkranz, P. W., Smith, W. L., Staelin, D. H., Strow, L. L. and Susskind, J., "AIRS/AMSU/HSB on the Aqua Mission: Design, Science Objectives, Data Products and Processing Systems," *IEEE Transactions on Geoscience and Remote Sensing*, **41.2**, 253-264, (2003).

[2] Aumann, H. H., Broberg, S. E., Elliott, D., Gaiser, S., and Gregorich, D., "Three years of Atmospheric Infrared Sounder radiometric calibration validation using sea surface temperatures," *JGR*, **111**, D16S90, doi:10.1029/2005JD006822, (2006).

[3] Ohring, G., Wielicki, B., Spencer, R., Emert, B., and Datla, R., "Satellite Instrument Calibration for Measuring Global Climate Change. Report of a Workshop," Bull. Am. Meteor. Soc., September (2005).

[4] Broberg, S. E., Pagano, T. S., Aumann, H. H., Elliott, D. A., and O'Callaghan, F., "Systems Approach to Developing a Climate Data Record from Satellite Observations," Proc. SPIE 7813 (2010).